Effects of α-particles on the resistive wall mode stability in ITER

Yueqiang Liu

Euratom/CCFE Fusion Association, Culham Science Centre, Abingdon, OX14 3DB, UK

E-mail contact of the author: yueqiang.liu@ccfe.ac.uk

abstract. The effects of the fusion born α particles on the stability of the RWM are numerically investigated for one of the advanced steady state Scenarios in ITER. The α contribution is found to be generally stabilising, compared to the thermal particle kinetic contribution alone. The same conclusion is achieved following both a perturbative and self-consistent approach. The latter generally predicts less stabilisation, than the former. At high enough plasma pressure, the self-consistent approach predicts two unstable branches for the ITER plasma studied here. The stabilising effect from α particles is found to be generally weak, in particular in terms of the modification of the stability boundary. The effect is more pronounced only at fast enough plasma rotation frequency, roughly matching the α precession frequency, which is in the order of a few percent of the toroidal Alfvén frequency for ITER. A simple, energy principle based, fishbone-like dispersion relation is proposed to gain a qualitative understanding of the numerical results.

1 Introduction

The steady state, 9MA scenario [1] in ITER aims at advanced plasma performance with high pressure and high bootstrap current fraction. The target plasma is designed to slightly exceed the Troyn no-wall beta limit [2]. The most significant concern for this plasma regime, from the macroscopic MHD point of view, is the stability (and possibly control) of the resistive wall mode (RWM) [3].

Because of its significance for ITER and power plants, the RWM has been extensively studied during recent years, both theoretically and experimentally. These efforts are well documented in a recent review article by Chu and Okabayashi [4]. Work has been carried out specifically on RWM modelling for ITER. In Ref. [5], rotational stabilisation and active control of the mode are investigated for the ITER advanced scenario, in the framework of the ideal MHD theory and a simplified drift kinetic damping model based on the mode resonance with the thermal particle bounce motion. This model predicts a critical toroidal plasma rotation speed of about 1.5-2% of the Alfvén speed in the plasma centre. The critical rotation speed is the minimal speed required for full suppression of the mode. A later model, based on the kinetic effects from the mode resonance with the thermal particle precession drifts, predicts that the RWM in ITER can be partially or fully stabilised, provided the plasma rotation frequency is below the ion diamagnetic frequency [6]. The calculations presented in [6] are for an ITER-like equilibrium but with an up-down symmetrised plasma boundary shape. A perturbative approach is pursued in this MHD-kinetic hybrid modelling, where the marginally stable, ideal kink mode eigenfunction is used to compute the drift kinetic energy. The ITER predictions, based on the self-consistent inclusion of the kinetic terms into the MHD equations, are made in recent studies [7, 8], but considering the thermal particle kinetic contributions only. Reference [7] mainly studies the effect of mode resonance with particle precession drifts, for realistic equilibria from the ITER design. Both perturbative and self-consistent approaches have been

used. Whilst the former predicts a full kinetic stabilisation of the RWM in a large region of the operational space, similar to [6], the latter approach predicts a smaller stabilisation domain, occurring at slow enough plasma flow. Reference [8] exploits a full gyrokinetic formulation to study the kinetic effects on the RWM for an ITER-like plasma, with a shallow magnetic shear reversal and an up-down symmetrised plasma shape. The thermal particle bounce resonances are included, which yields a rotation threshold of about 0.3% of the Alfvén speed.

This work focuses on the precessional resonance effects of trapped α particles on RWM stability in ITER. We compare the modelling results with and without the α contribution. As in [7], we follow both perturbative and self-consistent approaches, formulated in [9] for thermal particles, and in [10] for energetic particles, respectively. These formulations are implemented in the MARS-K code [9]. The same set of ITER equilibria as in [7] is used.

The following Section describes the model that we use for the α particles. Section 3 shows the MARS-K results of the RWM stability analysis, following the perturbative approach. Section 4 shows the MARS-K results based on the self-consistent kinetic formulation. Conclusions are drawn in Section 5.

2 Equilibrium properties of α particles

For the fusion born α particles, we assume an isotropic, slowing-down equilibrium distribution function [11]

$$f^0 = \begin{cases} \frac{C}{\varepsilon_k^{3/2}+\varepsilon_c^{3/2}} & 0 < \varepsilon_k < \varepsilon_\alpha \\ 0 & \varepsilon_k > \varepsilon_\alpha \end{cases} \tag{1}$$

where $\varepsilon_\alpha = 3.52\text{MeV}$ is the α birth energy, and

$$\varepsilon_c = \left(\frac{3\sqrt{\pi}}{4}\right)^{2/3} \left(\frac{M_\alpha}{M_i}\right) \left(\frac{M_i}{M_e}\right)^{1/3} T_e. \tag{2}$$

The quantities M_α, M_i, M_e denote the mass of α, thermal ions and electrons, respectively. The (thermal) electron equilibrium temperature is denoted as T_e.

The constant C from Eq. (1) is determined by giving the α density profile N_α. We use a profile predicted by the ASTRA simulation for the ITER 9MA steady state scenario. Figure 1 shows the radial profile of the ASTRA simulated α particle density and pressure profiles, normalised by the corresponding electron density and total thermal pressure. Note that the α particles contribute a fraction of about 20% of the thermal pressure in the plasma centre to the total equilibrium pressure, with only about 1% of the density fraction.

We point out two different assumptions made for the ITER plasma, between this study and the previous work [7]. First, this study assumes that both thermal (P_{th}) and α (P_α) particles contribute to the total equilibrium pressure $P_{\text{eq}} = P_{\text{th}} + P_\alpha$, whilst in [7], we have assumed that the total equilibrium pressure comes solely from the thermal ions and electrons $P_{\text{eq}} = P_{\text{th}}$ (i.e. no α particles are present in the plasma). In this work, we assume $P_{\text{eq}} = P_{\text{th}} + P_\alpha$ even when the *kinetic* contribution from α particles is excluded (i.e. the fluid potential energy is always

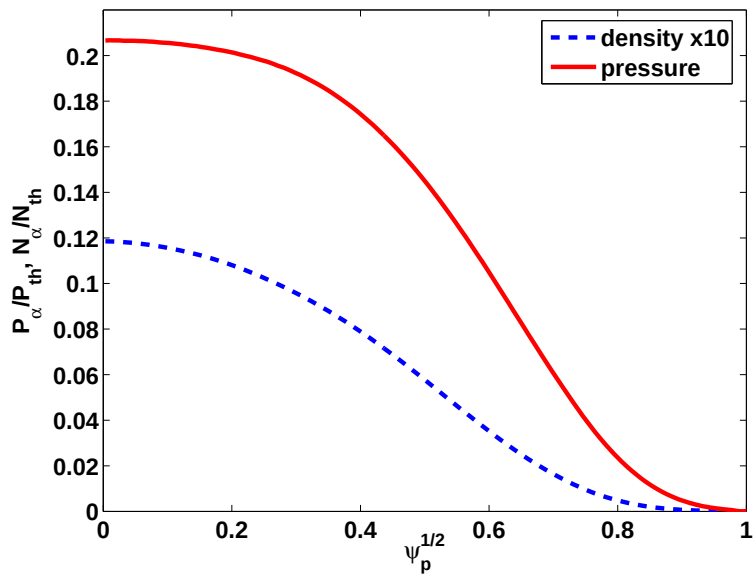

Figure 1: The radial profiles of the α particle density and pressure from the ASTRA simulation, normalised by the equilibrium electron density and the total thermal pressure, respectively. ψ_p is the equilibrium poloidal flux.

evaluated using the full equilibrium pressure P_{eq}). This allows us to clearly see the effect of the α contribution, compared to the thermal contribution alone. Secondly, the hydrogen thermal ions have been assumed in [7], whilst the DT reaction is assumed in this work (to produce the α particles).

In order to gain the physics insight into the mode-particle resonance, we show in Fig. 2 precessional drift frequencies of both trapped thermal ions and α particles, for one equilibrium with $C_\beta = 0.5$. [As in [7] and elsewhere, $C_\beta \equiv (\beta - \beta^{no-wall})/(\beta^{ideal-wall} - \beta^{no-wall})$ is defined as a linear scaling factor between the no-wall and the ideal-wall beta limits for the ideal external kink mode, such that $C_\beta = 0$ corresponds to the no-wall limit $\beta^{no-wall}$, and $C_\beta = 1$ corresponds to the ideal-wall limit $\beta^{ideal-wall}$]. Figure 2 shows that the α particles have an averaged precession frequency reaching 3% of the Alfvén frequency in the plasma core, and about 1% near the plasma edge. This frequency is about 35-100 times larger than the thermal ion precession frequency, and is consistent with the fact that the birth energy (3.52MeV) of the α particles is two orders of magnitude larger than the thermal ion kinetic energy in ITER. The α particle precession frequency is comparable to the amplitude of plasma toroidal rotation frequency. The radial profile, however, is rather different. The averaged precession frequency has a negative sign in the middle region along the minor radius, for both thermal and α particles. This is due to the precession reversal, enhanced by the finite pressure effect [12]. This sign reversal of the precession frequency for α particles has a significant consequence on the computed kinetic results, as will be demonstrated later in the paper. Finally we notice that the plasma toroidal rotation is normally treated as part of the toroidal precession drift for thermal or fast ions. We separate, however, the plasma rotation from the particle precession in this study.

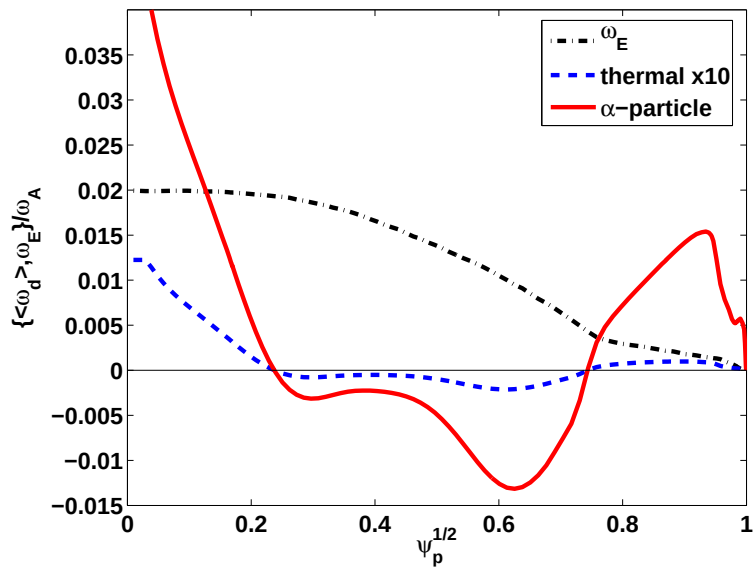

Figure 2: Comparison of the precessional drift frequencies, normalised by the Alfvén frequency, for the trapped thermal ions and α particles. The precession frequencies are an average of the particle equilibrium distributions over the velocity space and over the poloidal angle. Shown also the expected rotation profile ω_E for ITER, from Ref. [1]. ψ_p is the equilibrium poloidal flux. The ITER equilibrium [7] with $C_\beta = 0.5$ is considered.

3 Results with perturbative approach

In the perturbative approach, the drift kinetic modification of the RWM eigenfunction is neglected. In order to evaluate the perturbed drift kinetic energy, the eigenfunction of either an ideal kink mode at marginal stability [6], or fluid RWM [7], is used. The mode frequency (in the wall frame), that participates into the mode-particle resonance operator, is normally assumed to be either zero [6], or the fluid RWM mode frequency (as a complex number) [7]. The consequences of these different assumptions are discussed in [7]. As long as the plasma is not approaching the ideal-wall beta limit, these assumptions do not alter much the results of the perturbative approach. In the following, we shall use the fluid RWM eigenfunction and the (complex) mode frequency $\omega = i\gamma_f$ to evaluate the drift kinetic energy perturbations. Here γ_f is the growth rate of the fluid RWM in the absence of the plasma flow.

For RWM stability, normally two parameters play critical roles: the plasma pressure (C_β) and the plasma toroidal rotation frequency (ω_0 at centre). We first investigate the pressure effect at a fixed plasma rotation $\omega_0 = 0.02\omega_A$, where ω_A is the toroidal Alfvén frequency. This rotation frequency, probably with large uncertainties, is expected for the ITER steady state scenario [1].

Figure 3(a-b) compares the MARS-K computed drift kinetic energy perturbations (δW_k) versus C_β, with and without the α particle contribution. For comparison, the fluid potential energy, with and without an ideal wall, is also plotted. In the RWM regime, the fluid potential energy is negative (unstable) with the wall at infinity, and positive (stable) with an ideal wall. At this relatively fast plasma rotation, the α contribution significantly modifies the kinetic energy, compared to that with thermal particle contribution alone. The real part of total kinetic energy

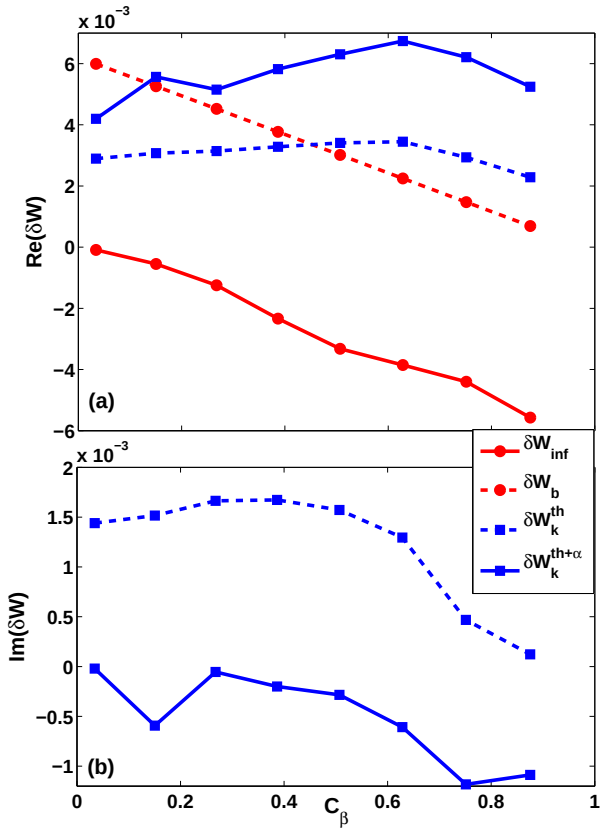

Figure 3: The (a) real and (b) imaginary parts of the perturbed fluid and drift kinetic energy with varying plasma pressure. The fluid potential energy is computed without wall ($\delta W_{\rm inf}$) and with an ideal ITER inner vacuum vessel (δW_b). The imaginary part of the fluid energy vanishes. The drift kinetic energy is computed using the fluid RWM eigenfunction, including the thermal particle contribution alone ($\delta W_k^{\rm th}$) or both thermal and α contributions ($\delta W_k^{\rm th+\alpha}$). All the energy terms are normalised by the plasma inertia associated with the displacement normal to the flux surface. The plasma toroidal rotation speed is assumed to be 2% of the Alfvén speed at the centre.

$\delta W_k^{\rm th+\alpha}$ is about two time larger than that of the thermal particle contribution alone $\delta W_k^{\rm th}$. The imaginary part is of about the same order by amplitude and with opposite signs. Whilst this reasonably strong effect from α particles will be qualitatively explained when Fig. 5 is discussed, we focus here on the fact that the kinetic energy perturbation, with the inclusion of the α contribution, becomes comparable to or larger than the fluid potential energy by amplitude. This leads to a substantial modification (stabilisation) of the RWM following the perturbative approach.

Figure 4 shows the RWM eigenvalue with increasing the plasma pressure, at a fixed plasma rotation frequency $\omega_0 = 0.02\omega_A$. The eigenvalue is calculated using the dispersion relation [13, 14]

$$\gamma\tau_w^* \simeq -\frac{\delta W_\infty + \delta W_k}{\delta W_b + \delta W_k}, \tag{3}$$

where τ_w^* is a normalisation factor related to the $n = 1$ field penetration time through the wall.

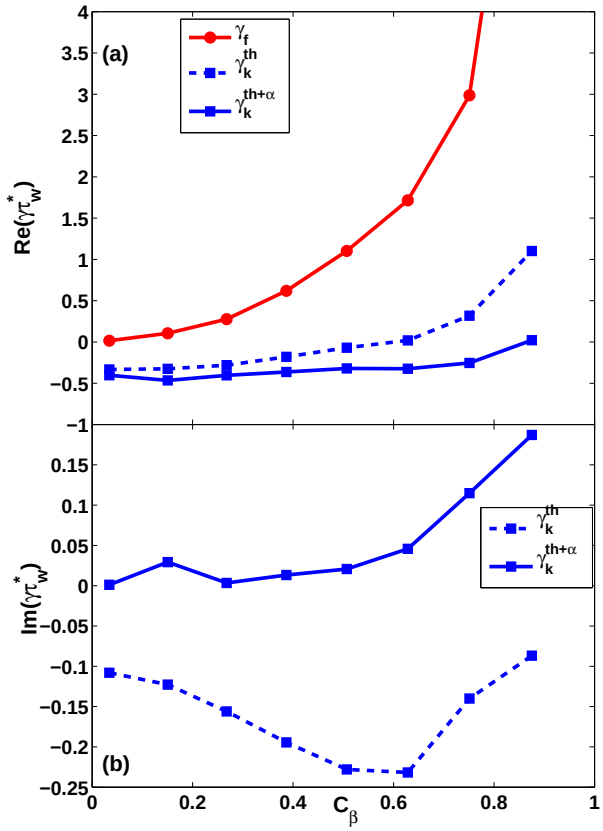

Figure 4: The (a) real and (b) imaginary parts of the RWM eigenvalue, normalised by the wall time and calculated using the RWM dispersion relation with the energy perturbations from Fig. 3. The eigenvalues with ($\gamma_k^{th+\alpha}$) and without (γ_k^{th}) the α contribution are compared. The fluid RWM growth rate (γ_f) for static plasmas is also shown in (a).

The fluid energy ($\delta W_\infty, \delta W_b$) and the drift kinetic energy ($\delta W_k = \delta W_k^{th}$ or $\delta W_k^{th+\alpha}$) are shown in the previous figure.

The significant effect is the full stabilisation, for all C_β values, of the mode by the α particles, following the perturbative approach. Without the α contribution, only a partial stabilisation of the mode is achieved - the mode is stable for $C_\beta < 0.55$ and unstable for $C_\beta > 0.55$. The α contribution also changes the sign of the mode rotation frequency (in the wall frame), without a significant modification of its magnitude.

The effect of the α particles on the kinetic energy and on the mode stability depends on the rotation frequency ω_0. Figure 5 shows the real and imaginary parts of δW_k versus ω_0, with and without the α contribution. The plasma pressure is fixed at $C_\beta = 0.5$. At very slow rotation ($\omega_0 = 2 \times 10^{-4}\omega_A$), the α contribution nearly vanishes. At the rotation speed close to the expected value for ITER ($\omega_0 \simeq 0.02\omega_A$), however, the α contribution does lead to a noticeable change of δW_k. A similar observation has been made in a recent study for a DIII-D plasma, where the beam-driven hot ions are modelled as the energetic particle source (also with an isotropic slowing down distribution) [10]. A qualitative, somewhat mathematical, explanation is obtained by examining the resonance operator, which has the following form for energetic

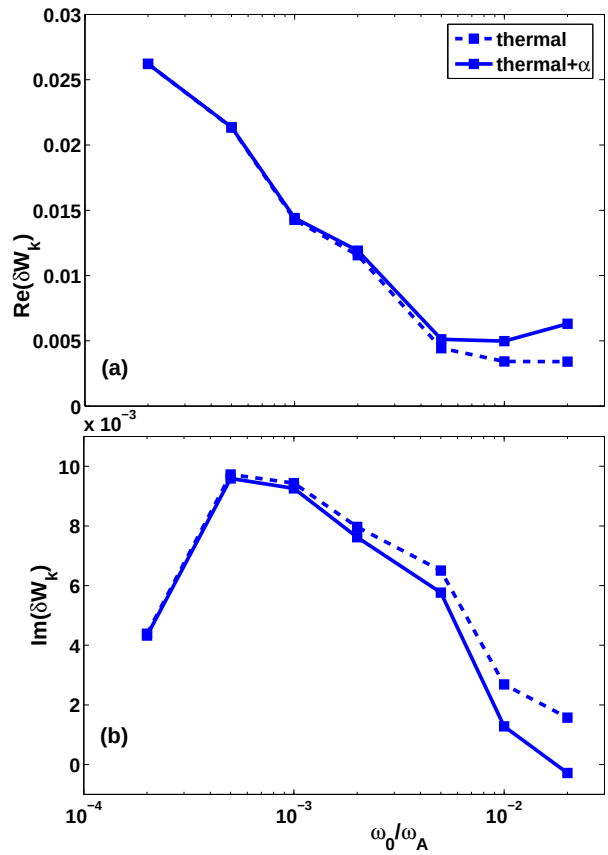

Figure 5: The (a) real and (b) imaginary parts of the perturbed drift kinetic energy with varying plasma central rotation speed. The energy is computed using the fluid RWM eigenfunction, including the thermal particle contribution alone (δW_k^{th}) or both thermal and α contributions ($\delta W_k^{\mathrm{th}+\alpha}$). All the energy terms are normalised by the plasma inertia associated with the displacement normal to the flux surface. The plasma pressure scaling factor is assumed $C_\beta = 0.5$.

particles

$$\frac{n\omega_E - \omega + n\omega_*^\alpha}{n\omega_E + n\omega_d^\alpha - \omega}, \tag{4}$$

where ω_* can be qualitatively interpreted as the diamagnetic frequency of fast ions (for more details see Eq. (10) from [10]). A careful comparison reveals that the ω_*^α term is typically two orders of magnitude larger than the ω_E term in the numerator of the expression (4), when $\omega_0 \equiv \omega_E(r=0) = 0.02\omega_A$. Therefore, the major contribution from the fast ions comes from a term like

$$\frac{n\omega_*^\alpha}{n\omega_E + n\omega_d^\alpha - \omega}. \tag{5}$$

Indeed, by running MARS-K with an artificial elimination of the ω_* term in (4), we found that the α particles barely modified the thermal particle results, for the whole rotation frequency range considered in this study.

If we neglect the mode frequency term ω in the expression (5), which is generally legitimate at fast enough plasma rotation, the behaviour observed in Fig. 5 can be explained as the interplay

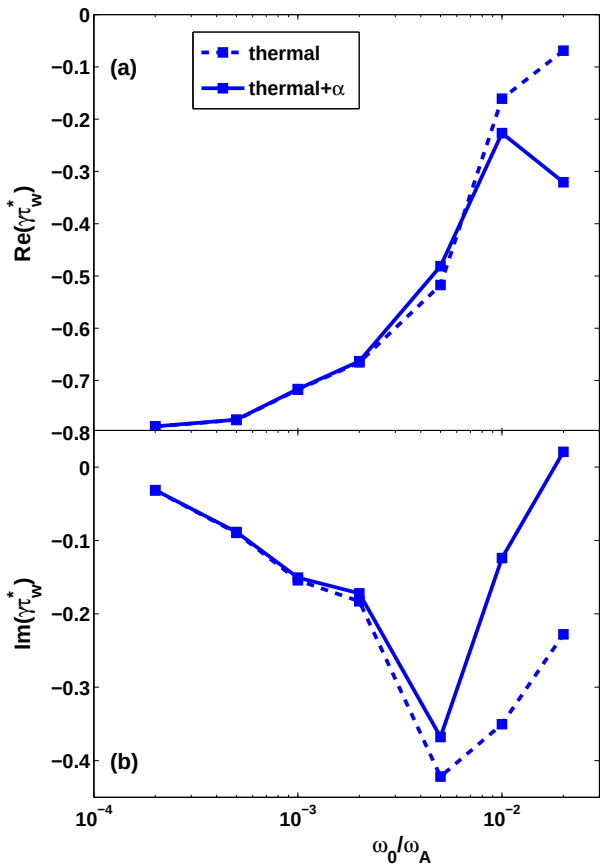

Figure 6: The (a) real and (b) imaginary parts of the RWM eigenvalue, normalised by the wall time and calculated using the RWM dispersion relation with the energy perturbations from Fig. 5. The eigenvalues with ($\gamma_k^{\mathrm{th}+\alpha}$) and without ($\gamma_k^{\mathrm{th}}$) the α contribution are compared. The plasma pressure scaling factor is assumed $C_\beta = 0.5$.

between ω_E and ω_d^α in the denominator of (5). The feature of the precession reversal for α particles, shown in Fig. 2, plays a crucial role. At slow rotation, $|\omega_E| << |\omega_d^\alpha|$, because of the sign reversal for ω_d^α (the sign of ω_* does not change), a significant cancellation occurs as the expression (5) is integrated (together with other multipliers) over the minor radius. A fast enough plasma rotation, however, tends to eliminate the precession reversal of fast ions, and hence reducing the cancellation effect during the radial integration.

The behaviour of δW_k versus the plasma rotation speed is reflected in the subsequent stability analysis following the dispersion relation (3), as shown in Fig. 6. At slow plasma rotation ($\omega_0 \lesssim 2\times 10^{-3}\omega_A$), the α kinetic contribution is very small. At fast rotation ($\omega_0 \rightarrow 0.02\omega_A$), the α particles cause the mode to be more stable. The mode frequency changes sign only at fast enough plasma rotation.

The α particle effect on the mode stability has also been examined in the 2D space of (ω_0, C_β). Figures 7(a-b) compare the real part of the RWM eigenvalue, with and without the α contribution, following the perturbative approach. We notice that, despite different assumptions for the plasma thermal particles, the stability boundary shown in Fig. 7(a) is close to that obtained in figure 15(a) from Ref. [7]. The perturbative approach predicts that the precession drift ki-

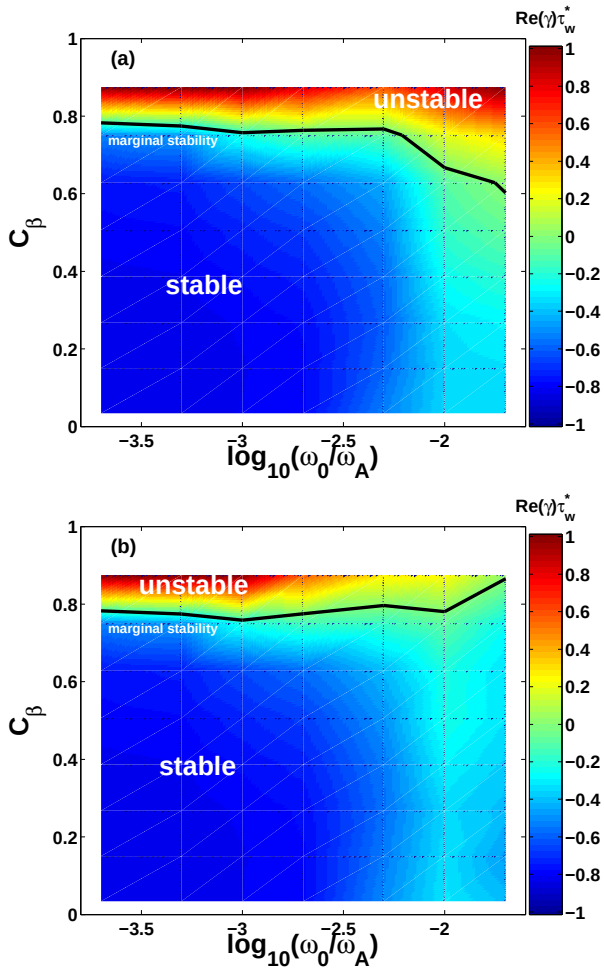

Figure 7: Contour plots of the real part of the normalised RWM eigenvalue with varying plasma pressure and rotation speed. The perturbative approach is used to compute the eigenvalue for the case (a) with the thermal particle drift kinetic contribution alone, and case (b) with both thermal and α contributions. The solid lines indicate the stability boundary.

netic effect of α particles is generally stabilising for the RWM. The effect becomes stronger as the plasma rotation speed increases. The mode remains unstable at high pressure $C_\beta \gtrsim 0.8$ and slow plasma rotation ($\omega_0 \lesssim 4 \times 10^{-3}\omega_A$), even with the inclusion of the α effect. As a result, the α contribution expands the stable domain for the RWM, but does not completely stabilise the mode across the full parameter domain. In terms of the modification of the stability boundary, the α effect is rather weak compared to that of the thermal particle effects.

4 Results with self-consistent approach

The self-consistent approach solves the MHD equations together with the drift kinetic integrals, in a MHD-kinetic hybrid manner [9, 10]. There are two major differences compared with the perturbative approach: (i) the mode eigenfunction is allowed to be modified by the

kinetic effects in the self-consistent approach; (ii) the unknown mode eigenvalue γ enters also into the kinetic integrals in a nonlinear fashion. These differences can have a large impact on the prediction for the kinetic RWM stability.

Figure 8 compares the MARS-K computed mode eigenvalue, with and without the α contribution, following the self-consistent approach. We vary the plasma rotation frequency while fixing the pressure at $C_\beta = 0.63$. In both cases, with or without the α contribution, there are two unstable branches (solid and dashed lines). The α particles have a stabilising effect on both branches. For the first unstable branch (dashed lines), the α effect is weak at slow plasma rotation; probably for the same reason as discussed in the previous Section. For both branches, the α stabilisation is more significant at sufficiently fast rotation $\omega_0 \rightarrow 2 \times 10^{-2}\omega_A$. Note that this is the same frequency range for the precessional drifts of α particles (Fig. 2). The local minimum in the first branch, as well as the marginal stability for the second branch (solid lines), corresponds to $\omega_0 \sim 10^{-3}\omega_A$. This is roughly the precession frequency for thermal particles.

Similar results have been obtained for a DIII-D plasma [10], where the fast particles are the beam driven hot ions. Because of the co-existence of both unstable branches, the overall (i.e. the maximum of two growth rates) mode remains unstable for this plasma, with or without the α contribution.

The mode frequency for the second branch remains small with varying the plasma rotation. The mode frequency for the first branch increases linearly with ω_0, reaching a value of about $7 \times 10^{-3}\omega_A$ at $\omega_0 = 2 \times 10^{-2}\omega_A$. The α contribution does not significantly modify this frequency behaviour. We mention that similar behaviour for the first unstable branch is also observed for two other high beta plasmas with $C_\beta = 0.88$ and 0.75.

Both branches shown in Fig. 8 have a global, kink-like eigenmode structures. Figures 9(a-c) plot three sets of eigenfunctions, for three chosen points from Fig. 8. The radial profiles of the poloidal Fourier harmonics for the radial displacement are compared, with and without the α contribution. At slow plasma rotation (case (a)), the α particles do not modify the mode eigenfunction, in agreement with the fact that the mode eigenvalue is also not changed. Faster plasma rotation (cases (b-c)) leads to slightly larger α modification of the mode structure. This modification is small but global.

The co-existence of two unstable branches occurs only at sufficiently high plasma pressures. Figure 10 scans C_β at fixed plasma rotation frequencies, for the first branch at slow rotation (dashed lines) and the second branch at fast rotation (solid lines). The first unstable branch quickly becomes stable as the plasma pressure drops. The second branch, on the contrary, remains unstable through a large part of the pressure range (for the rotation frequency of $\omega_0 = 2 \times 10^{-2}\omega_A$). The α contribution is again stabilising in all cases.

The RWM stability diagrams from a 2D parameter ($\omega_0 - C_\beta$) scan are shown in Figs. 11(a-b). The diagrams are compared with and without the α particle contribution. Figure 11(a) agrees roughly with Fig. 15(b) from Ref. [7], even though somewhat different assumptions have been made for the equilibrium plasma. Comparing Figs. 11(a) and (b), we find that the α contribution slightly extends the stability boundary (towards higher beta) at high rotation. At slow rotation, the stability boundary is not modified by α particles, as should be expected. However, the mode growth rate is substantially reduced by α particles at high beta and fast

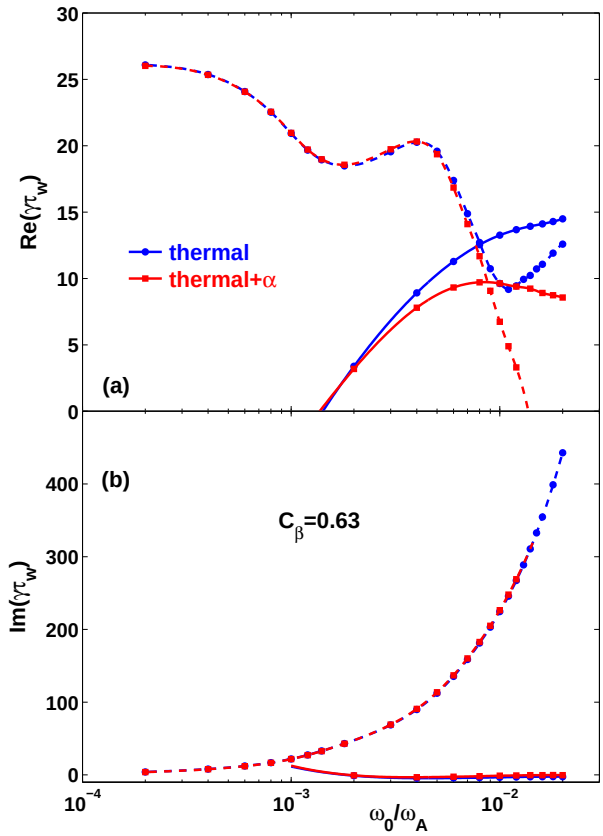

Figure 8: The (a) real and (b) imaginary parts of the RWM eigenvalue, normalised by the wall time and computed following the self-consistent approach. The eigenvalues with (filled square) and without (filled dot) the α contribution are compared. The first unstable branch (dashed) and the second unstable branch (solid) are shown. The plasma pressure scaling factor is $C_\beta = 0.63$.

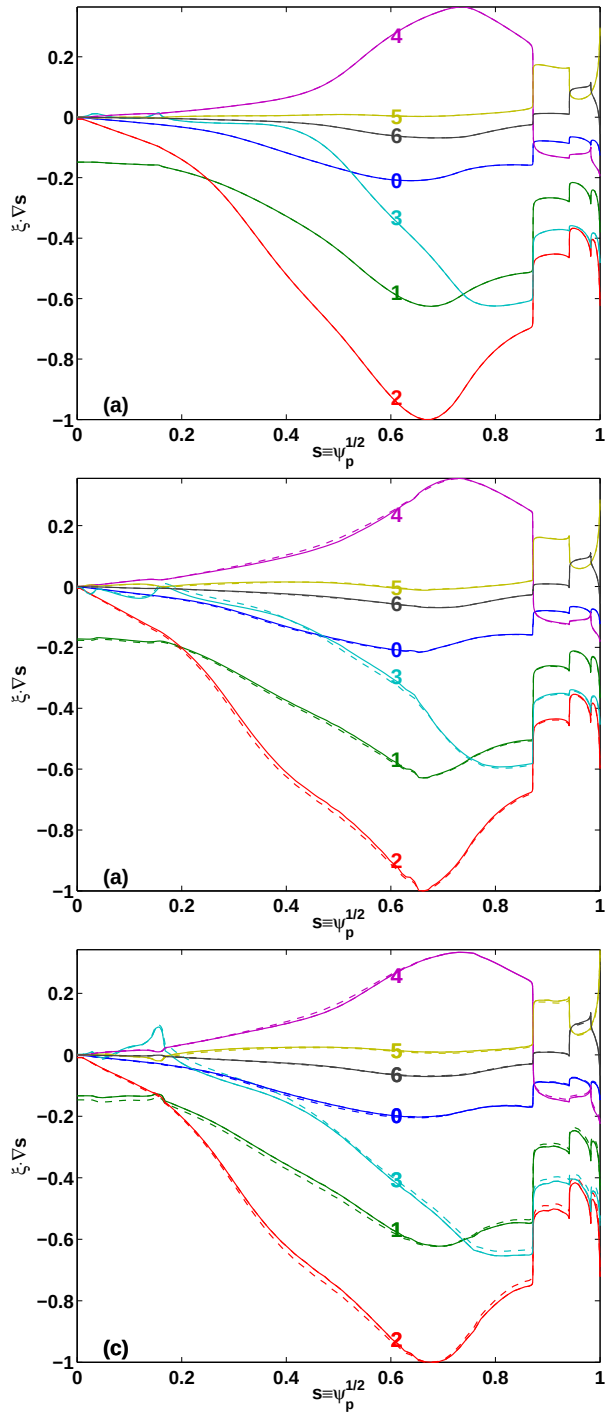

Figure 9: The poloidal harmonics of the radial displacement, corresponding to cases shown in Fig. 8 for (a) the first branch at $\omega_0 = 2 \times 10^{-4}\omega_A$, (b) the first branch at $\omega_0 = 1.2 \times 10^{-2}\omega_A$, and (c) the second branch at $\omega_0 = 2 \times 10^{-2}\omega_A$. The eigenfunctions are compared with (solid) and without (dashed) the α contribution. Shown only the dominant harmonics $m = 0, \cdots, 6$, indicated in the figure. An equal-arc flux coordinate system is used.

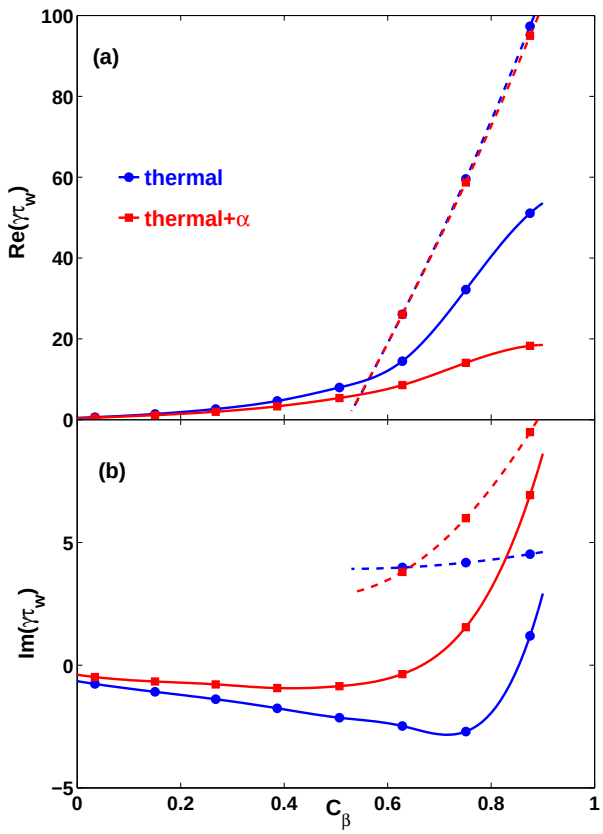

Figure 10: The (a) real and (b) imaginary parts of the RWM eigenvalue, normalised by the wall time and computed following the self-consistent approach. The eigenvalues with (filled square) and without (filled dot) the α contribution are compared. Shown are the eigenvalues for the first unstable branch at $\omega_0 = 2 \times 10^{-4}\omega_A$ (dashed) and for the second unstable branch at $\omega_0 = 2 \times 10^{-2}\omega_A$ (solid).

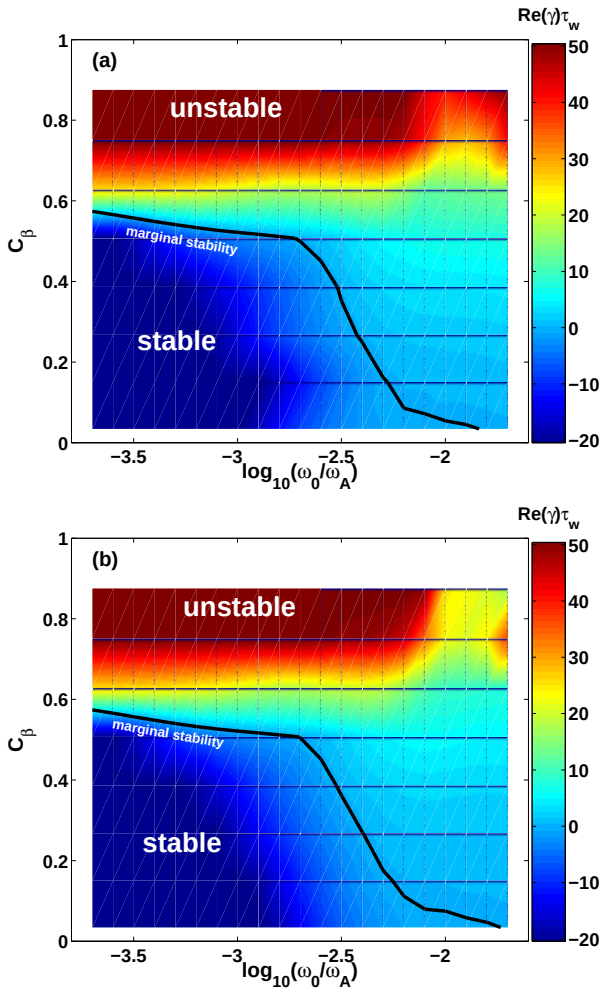

Figure 11: Contour plots of the real part of the normalised RWM eigenvalue with varying plasma pressure and rotation speed. The self-consistent approach is used to compute the eigenvalue for case (a) with the thermal particle drift kinetic contribution alone, and case (b) with both thermal and α contributions. The maximal growth rate is taken when there are two unstable branches of the solution. The solid lines indicate the stability boundary.

rotation.

The α particle effect obtained in the above self-consistent numerical computations can be qualitatively understood with the following simple dispersion relation

$$D(\gamma) \equiv \delta W_p + \frac{\delta W_v^{\infty} + \gamma \tau_w^* \delta W_v^b}{1 + \gamma \tau_w^*} + C_h \Omega \ln\left(1 - \frac{1}{\Omega}\right) = 0, \tag{6}$$

where $\Omega \equiv \omega/\omega_d = i\gamma/\omega_d$. In the above dispersion relation, the first term δW_p in $D(\gamma)$ is the fluid potential energy associated with the plasma. We assume here that the equilibrium pressure contribution to δW_p comes only from the thermal pressure [15]. The second term in $D(\gamma)$ is associated with the vacuum energy. [The inertia is neglected assuming that the amplitude of the mode eigenvalue γ is much smaller than the Alfvén frequency ω_A.] The last term of $D(\gamma)$ is due to the α contribution. This term can be obtained in a similar way as in the fishbone theory for hot ions [15], neglecting the plasma rotation. The coefficient C_h is

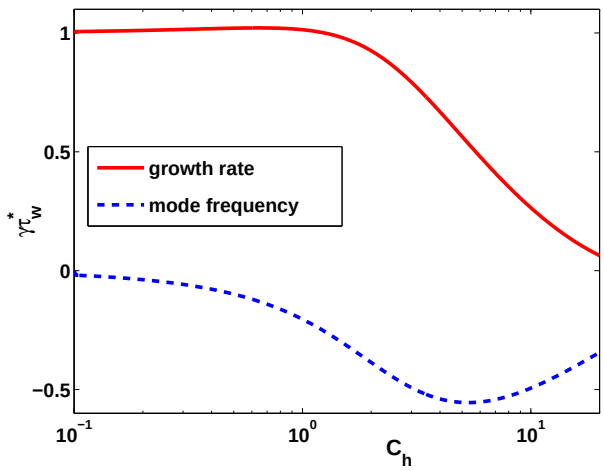

Figure 12: The unstable root of the dispersion relation (6) versus the hot ion pressure parameter C_h. The other parameters in this example are assumed as $\delta W_p = -1, \delta W_v^\infty = 0.5, \delta W_v^b = 1.5, \tau_w^* = 10^4 \tau_A, \omega_d = 10^{-2}\omega_A$.

proportional to the hot ion pressure. We treat it as a free parameter in this qualitative analysis.

Figure 12 shows an example of the root tracing versus C_h for the dispersion relation (6). The parameters are chosen such that the growth rate of the fluid RWM (without the α contribution, $C_h = 0$), normalised by the wall time τ_w^*, is unity. Increasing the α contribution, the mode is initially slightly destabilised, followed by a strong stabilisation at large values of C_h. Comparison of this simple model with the numerical results indicates that the ITER parameter regime corresponds to a large value of C_h, whilst the DIII-D plasma (numerical results presented in Ref. [10]) seems to be in the small C_h regime.

We mention that the dispersion relation (6) also allows a second unstable root for certain parameter range. For the parameter set as in Fig. 12, the second unstable root appears in a narrow range of $C_h \in [0.042, 0.5]$. This can be easily shown by plotting the Nyquist diagram of the function $D(i\omega)$. This second unstable root generally has a smaller growth rate than the one shown in Fig. 12, but a large mode frequency, close to the hot ion precessional drift frequency ω_d. This root is the fishbone equivalent for the kinetic RWM. This high frequency, unstable root bears some similarity to the first unstable branch shown in Fig. 8.

5 Conclusions

The effects of the fusion born α particles on the stability of the RWM are numerically investigated using the MARS-K code, for the ITER steady state scenario given by Ref. [1].

For the ITER plasma regime, the α contribution is generally more stabilising, than the thermal particle kinetic contribution alone. The same conclusion is achieved following both the perturbative and the self-consistent approaches. The latter generally predicts less stabilisation than the former. With the ASTRA predicted α density and pressure profiles, the stabilising effect from the α particles is generally weak.

At high enough plasma pressure, the self-consistent approach yields two unstable branches, both having a global kink mode structure. As expected, the stabilising effect from the α particles becomes more pronounced only at fast enough plasma rotation frequency, roughly matching the α precession frequency. For the ITER plasma, this is in the order of a few percent of the toroidal Alfvén frequency.

A simple, energy principle based (self-consistent) dispersion relation is proposed to gain a qualitative interpretation of the numerical results.

The modelling presented here neglects the effect of finite drift orbit width (the banana width) of trapped α particles, which is expected to be reasonably large compared to the plasma minor radius in ITER. For a mode with global eigenmode structure, the finite banana width effect may not be critical from the qualitative point of view. Nevertheless, a realistic modelling requires inclusion of this effect, by using, e.g. the HAGIS code [16].

Acknowledgements

The author would like to thank Dr. A. Polevoi for providing detailed information on the ASTRA model for the α density. The author also thanks Dr. T.C. Hender for careful reading of the manuscript and for helpful comments and suggestions.

This work was funded by the United Kingdom Engineering and Physical Sciences Research Council under grant EP/G003955 and the European Communities under the contract of Association between EURATOM and CCFE. The views and opinions expressed herein do not necessarily reflect those of the European Commission.

References

[1] Polevoi A. *et al* *Proc. 19th Int. Conf. on Fusion Energy 2002 (Lyon, France, 2002)* (Vienna: IAEA) CD-ROM file CT/P-08 and http://www.iaea.org/programmes/ripc/physics/fec2002/html/fec2002.htm

[2] Troyn F. *et al* 1984 *Plasma Phys. Control. Fusion* **26** 209

[3] Hender T.C. *et al* 2007 *Nucl. Fusion* **47** S128

[4] Chu M.S. and Okabayashi M. 2010 *Plasma Phys. Control. Fusion* at press

[5] Liu Y.Q. *et al* 2004 *Nucl. Fusion* **44** 232

[6] Hu B., Betti R. and Manickam J. 2005 *Phys. Plasmas* **12** 057301

[7] Liu Y.Q. *et al* 2009 *Nucl. Fusion* **49** 035004

[8] Zheng L.J., Kotschenreuther M.T. and Van Dam J.W. 2009 *Nucl. Fusion* **49** 075021

[9] Liu Y.Q. *et al* 2008 *Phys. Plasmas* **15** 112503

[10] Liu Y.Q. *et al* 2010 *Plasma Phys. Control. Fusion* at press

[11] Hu B., Betti R. and Manickam J. 2006 *Phys. Plasmas* **13** 112505

[12] Connor J.W., Hastie R.J. and Martin T.J. 1983 *Nucl. Fusion* **23** 1702

[13] Haney S.W. and Freidberg J.P. 1989 *Phys. Fluids B* **1** 1637

[14] Chu M.S. *et al* 1995 *Phys. Plasmas* **2** 2236

[15] Chen L., White R.B. and Rosenbluth M.N. 1984 *Phys. Rev. Lett.* **52** 1122

[16] Pinches S.D. *et al* 1998 *Comput. Phys. Commun.* **111** 133